

Video Article

Laser Nanosurgery of Cerebellar Axons *In Vivo*

Anna L. Allegra Mascaro¹, Leonardo Sacconi^{1,2}, Francesco Saverio Pavone^{1,2,3,4}¹European Laboratory for Non-Linear Spectroscopy, University of Florence²National Institute of Optics, National Research Council³Department of Physics and Astronomy, University of Florence⁴International Center for Computational Neurophotonics (ICON Foundation)Correspondence to: Anna L. Allegra Mascaro at allegra@lens.unifi.itURL: <http://www.jove.com/video/51371>DOI: [doi:10.3791/51371](https://doi.org/10.3791/51371)Keywords: Neuroscience, Issue 89, axonal labeling, neuronal tracing, *in vivo* imaging, two-photon microscopy, cerebellum, climbing fibers, laser axotomy, craniotomy

Date Published: 7/28/2014

Citation: Allegra Mascaro, A.L., Sacconi, L., Pavone, F.S. Laser Nanosurgery of Cerebellar Axons *In Vivo*. *J. Vis. Exp.* (89), e51371, doi:10.3791/51371 (2014).

Abstract

Only a few neuronal populations in the central nervous system (CNS) of adult mammals show local regrowth upon dissection of their axon. In order to understand the mechanism that promotes neuronal regeneration, an in-depth analysis of the neuronal types that can remodel after injury is needed. Several studies showed that damaged climbing fibers are capable of regrowing also in adult animals^{1,2}. The investigation of the time-lapse dynamics of degeneration and regeneration of these axons within their complex environment can be performed by time-lapse two-photon fluorescence (TPF) imaging *in vivo*^{3,4}. This technique is here combined with laser surgery, which proved to be a highly selective tool to disrupt fluorescent structures in the intact mouse cortex⁵⁻⁹.

This protocol describes how to perform TPF time-lapse imaging and laser nanosurgery of single axonal branches in the cerebellum *in vivo*. Olivocerebellar neurons are labeled by anterograde tracing with a dextran-conjugated dye and then monitored by TPF imaging through a cranial window. The terminal portion of their axons are then dissected by irradiation with a Ti:Sapphire laser at high power. The degeneration and potential regrowth of the damaged neuron are monitored by TPF *in vivo* imaging during the days following the injury.

Video Link

The video component of this article can be found at <http://www.jove.com/video/51371/>

Introduction

Axonal transection resulting from mechanical injury, toxic insult or neurodegenerative diseases is usually followed by degeneration of the distal part of the axon that is detached from the cell body¹⁰⁻¹³. With a few exceptions^{2,7,14,15}, severed axons in the CNS of adult animals are usually unable to activate a regrowth program¹⁶.

Little is known about the real-time dynamics of degenerative events at the cellular and subcellular level. The development of new strategies for limiting neuronal damage and promoting neuronal regrowth requires, as a first step, clarifying the mechanism by which singularly injured neuronal cells degenerate and regenerate. This study is most directly addressed by monitoring the dynamics of a single neuron *in vivo*. While one-photon fluorescence imaging techniques are limited by intense scattering of visible light, two-photon excitation reaches deep cortical layers in live mice with subcellular resolution^{3,4,17}. Taking advantage of transgenic mice in which fluorescent proteins are selectively expressed in subpopulations of neurons¹⁸⁻²⁰, TPF microscopy has been applied to the exploration of synaptic plasticity and axonal elongation during development *in vivo*^{21,22}. The capability of singularly damaged neurons to regrow after injury can be investigated by coupling *in vivo* monitoring by two-photon imaging with a model of injury specifically targeted to the axon of interest. Multi-photon absorption of femtosecond pulses has been used to disrupt single dendrites or even single spines^{5,23}. Moreover, this injury paradigm allows cutting single axonal branches without disrupting the contacting dendrite⁶. Within the context of dissecting the features that allow specific neuronal population to regenerate their axons once damaged, cerebellar climbing fibers (CFs) are a useful model since they retain remarkable plastic properties after injury even in adult animals^{24,25}. Recently, long-term imaging of CFs showed that these axons are capable of regrowing in the days that follow laser axotomy⁵.

This protocol describes how to label olivocerebellar neurons and their axonal elongation through anterograde tracing. Once the neurons of interest are fluorescently labeled, they can be monitored repeatedly at arbitrary time points for weeks or months under a cranial window. The procedure to dissect single axonal branches by laser axotomy *in vivo* will then be illustrated.

The techniques presented here provide new insights into the mechanism of axonal remodeling *in vivo* and may help the development of therapeutic strategies to limit neuronal degeneration and promote axonal regrowth.

Protocol

1. Axonal Labeling

1. Climbing fibers can be labeled by injecting either organic dyes conjugated to high molecular weight dextrans or plasmid/viruses that induce the expression of fluorescent proteins²⁶⁻²⁹. In this protocol, the organic dye Alexa Fluor Dextran 488 is injected into the inferior olive to label climbing fibers and visualize them in the cerebellar cortex (**Figure 1**). All the procedures described here have been approved by the Italian Ministry of Health.
2. Prepare the glass capillary tube by pulling it on a micropipette puller. Trim the tip of the glass capillary tube with scissors till the external diameter is about 30 μm .
3. Load the capillary with 1-2 μl of the dextran-conjugated dye.
4. Before starting, sterilize all the surgical instruments in an autoclave. During the procedure, reduce risks of contamination by using a glass bead sterilizer.
5. Anesthetize the mouse (9-12 weeks) by intraperitoneal injection of ketamine (90 mg/kg) and xylazine (9 mg/kg). Ensure the animal is fully sedated using tail and/or toe pinches. Use vet ointment on eyes to prevent dryness while under anesthesia.
6. Shave the hairs above the neck with either a razor blade or hair removal cream. Swab the surgical site twice with betadine, alternated with ethanol 70%.
7. Place the mouse on a stereotaxic holder. Keep the animal warm with a heating pad.
8. Gently push the earbars on the bone next to the ears so that the head is held firmly. Rotate the head to form a 140° angle with the body. The desired orientation can be obtained by gently changing the height of the nose holder rod on the stereotaxic holder.
9. Apply some drops of lidocaine on the skin between the ears. Use forceps or a razor blade to perform a vertical incision of about 1 cm on the skin below the occiput.
10. Gently separate the subcutaneous tissue and muscles by blunt tweezers under the dissection microscope. Push down the horizontal muscle bundle and hold apart the two vertical muscles fascicles in order to expose the dura over the foramen magnum.
11. Using extreme caution, dissect the dura with a syringe needle or very sharp forceps to expose the brainstem. A small quantity of cerebrospinal fluid may spill out when the dura has been cut.
12. On the stereotaxic micromanipulator, rotate the holder of the capillary 45° from the vertical. Place the capillary at the midline, at the midpoint between the caudal edge of the cerebellar cortex and the first cervical vertebra. Insert the pipette at a depth of 2 mm from the surface.
13. Deliver a 0.5-1.5 μl volume of dye over 10-15 min. A microinjection dispensing system allows controlled pressure delivery of the liquid in the capillary (Pulse pressure = 20 psi; pulse duration = 3-4 msec; frequency of pulse delivery = 12 Hz).
14. Leave the capillary in place for 15 min, then slowly (in 2-3 min) remove it. Delicately re-align the muscles and suture the skin above. Keep the muscles well hydrated by applying some saline throughout the whole procedure.
15. To avoid dehydration, inject subcutaneously 0.5 ml of 0.9% NaCl. Keep the animal in a heated cage until full recovery from anesthesia.
16. Subcutaneously administer Carprofen (5 mg/kg) daily for 2-3 days after the surgery.

2. Optical Window on the Cerebellar Cortex

NOTE: The dye is transported in 2 weeks from the inferior olivary nucleus up to the cerebellar cortex to the CFs terminals (see **Figure 1**). The sparsely labeled CFs can be visualized under the permanent cranial window that can be performed as follows:

1. Sterilize all the surgical instruments.
2. Anesthetize the mouse as described above. Use toe pinches to check the animal is fully sedated.
3. Shave the hair above the head, wipe the skin with alternating swipes of 70% alcohol and betadine and apply eye ointment. Place the mouse in a stereotaxic frame and position the ear bars in order to firmly hold the head.
4. Subcutaneously administer Dexamethasone (0.2 mg/kg) and Carprofen (5 mg/kg) to prevent swelling of the brain and possible inflammations at the cranial window site.
5. Apply a drop of lidocaine on the skin above the skull and cut a flap, from between the ears to above the eyes. Apply lidocaine solution again onto the periosteum before scraping it with a scalpel.
6. Use the dental drill to thin a semicircular region of skull above the cerebellum. The window is usually placed central and towards the back suture, so that the skull depth is almost constant throughout the perimeter of the semicircle. Positioning the window too close to the lambda suture and repetitive drilling over this very thick region may result in overheating of the brain and formation of edemas.
7. Apply hemostatic sponge on the skull in case of bleeding.
8. Cut a coverglass in two halves with the help of a razor blade and tweezers. Check that the coverglass is slightly bigger than the isle of bone and has a similar shape before removing the flap of bone with the tweezers; if not, reshape the coverglass or choose another one. Do not touch the dura mater with the tweezers while drawing off the bone. Carefully lay down the coverglass upon the dura. NOTE: The adherence of the whole surface of the glass on the dura is foretelling of long lasting cranial windows.
9. Remove air bubbles under the glass by repeatedly rinsing with saline solution and drying with cotton sticks. This will also help removing some residual blood that might be spilled out from small capillaries after positioning the glass. Seal the window with a mixture of acrylic glue and dental cement³⁰.
10. Keep the animal on a heating pad in a recovery chamber until fully recovered from anesthesia. Do not return mice in the home cage until fully recovered; do not leave them unattended until they regained sufficient consciousness to maintain sternal recumbency.
11. Subcutaneously administer Carprofen (5 mg/kg) daily for 2-3 days after the surgery.

3. *In Vivo* Multi-photon Laser Axotomy

1. Wait 2-7 days from the surgery before performing the first imaging session. The custom built two-photon microscope used here is provided with a Ti:Sapphire laser source (120 fs width pulses, 90 MHz repetition rate) which is first scanned by a pair of galvanometric mirrors and then focused onto the specimen by a water immersion 20X objective (NA 0.95, WD 2 mm). A closed-loop piezoelectric stage performs axial displacements up to 400 μm of the objective. Photomultiplier tubes collect the fluorescence signal.
2. Anesthetize the animal, then position the head in the stereotactic holder so that the cranial window lays parallel to the objective focal plane.
3. Explore with TPF imaging the cortex under the cranial window. Choose the axon to be damaged amongst the brightest ones.
4. Acquire a Z-stack (usually the field of view is 100 x 100 μm^2 , at 512 x 512 pixels, 2 μm z-axis step) to obtain a 3D-reconstructions of the targeted axon. Within the imaged volume, choose the lesion site on an axonal branch that lies mostly parallel to the focal plane. This orientation allows to rapidly score morphological changes, which are predictive of a successful dissection.
5. Irradiate with a high energy dose the selected point on a distal portion of a CF. This is done through the Labview software: increase the laser power 5-10x more than the power used for imaging (\approx 300 mW, measured after the objective lens), set the position of the galvanometric mirrors to do a line scan (\sim 4-10 μm) on the lesion site and open the laser shutter for 400 - 600 msec. Orientate the line scan perpendicular to the CF plane to completely transect the axon. Irradiating brighter spots (e.g., varicosities) usually helps dissecting the axon. The wavelength for laser axotomy is the same used for imaging (920 nm).
6. Usually the fluorescence of the axon in the irradiated area transiently decreases due to photobleaching. Acquire a stack of the same region few minutes after the irradiation to ensure the ablation has been well performed. If the region started swelling and the axon formed bead-like structures, the neuron has been successfully dissected. In this case, in a few hours (from few tens of min to 24 hr) the distal portion of the axon will degenerate and disappear completely.
7. Unfortunately the energy dose necessary to produce a complete axotomy is not always predictable. If the only outcome of the irradiation is photobleaching, the fluorescence should be rapidly recovered due to dye diffusion, and the irradiation should be repeated again to effectively dissect the axon. Also, in case signs of swelling do not appear within 5 - 20 min, or the swelling is followed by recovery (analogously to what has been described for laser dendrotomy, see Allegra Mascaro *et al.*²³), try again with new scans increasing the dwell time and/or the laser power.
8. Monitor the eventual remodeling of the axon in the days that follow the laser axotomy with two-photon *in vivo* imaging (**Figures 2 and 3**). The vascular pattern is used as reference pattern to retrieve the dissected axon in the following days.
9. Subcutaneously administer Carprofen (5 mg/kg) every imaging session for the whole duration of the experiment.

Representative Results

This protocol described how to perform axonal labeling, *in vivo* imaging and laser axotomy on single neurons. The timeline of the experiment is shown in **Figure 1**.

An example of CFs labeled with Alexa Fluor 488 Dextran and visualized under the cranial window by *in vivo* two-photon microscopy is reported in **Figure 2**. As previously reported^{6,27}, the ascending branches display a high stability throughout the observation period of several days.

Figure 3 shows an example of axonal severing by laser axotomy of a single branch of a CF. As previously described, the damage was performed by irradiating a distal branch (\sim 30 μm below the pia) of a CF with a high energy dose of infrared light. As shown in the second panel of **Figure 3**, 15 min after laser irradiation the distal portion of the axon started swelling and degenerating. The day after, the portion of the axon distal to the lesion site completely disappeared (**Figure 3**, d17). The degenerated portion is highlighted by the red arrowheads in the time course. The last two panels also show the progressive formation of a new transverse branch (green arrowhead) from the injured axon (more details on the sprouting of new branches after laser axotomy *in vivo* can be found in⁶).

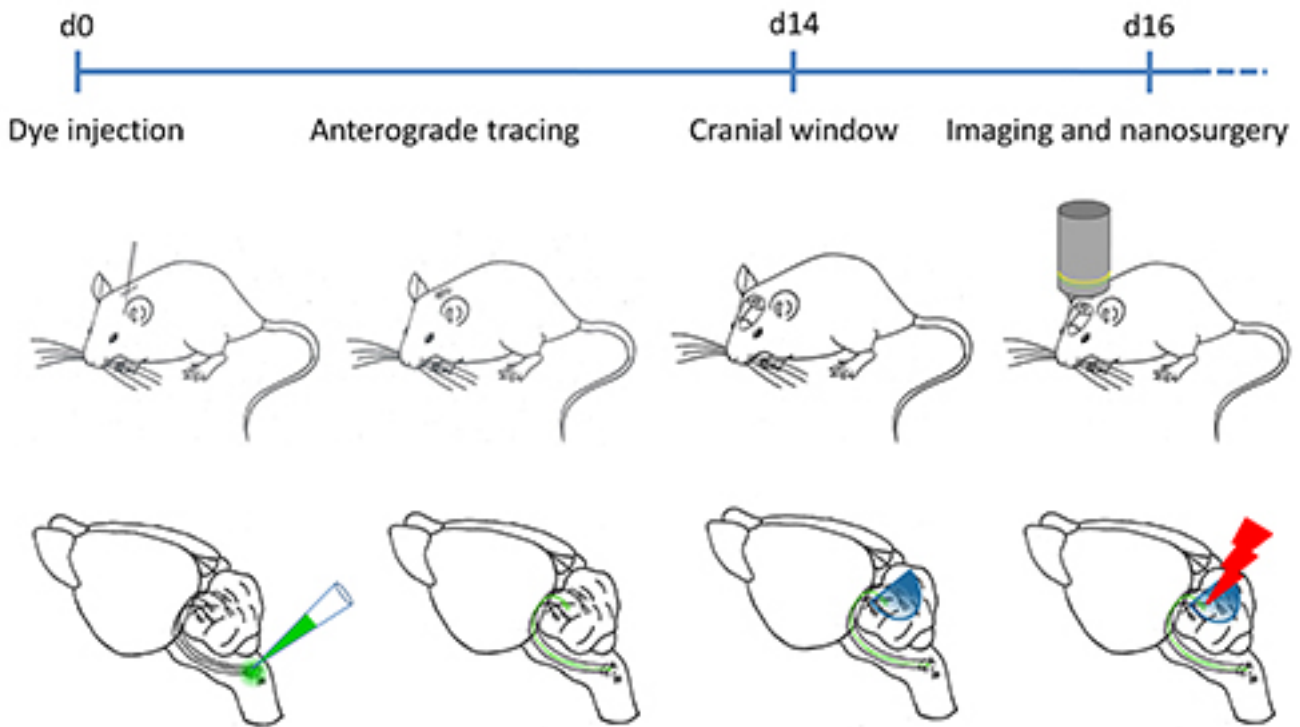


Figure 1. Timeline of the laser nanosurgery experiment. After the injection into the inferior olivary nucleus, two weeks of recovery will allow the anterograde dextran-conjugated dye to label the climbing fibers. The cerebellar cortex is then exposed by performing a permanent cranial window. From 2-7 later on, the labeled CFs can be imaged under the two-photon microscope *in vivo* at arbitrary time intervals. The laser nanosurgery on the labeled axons can be performed at any time after the cranial window has been implanted.

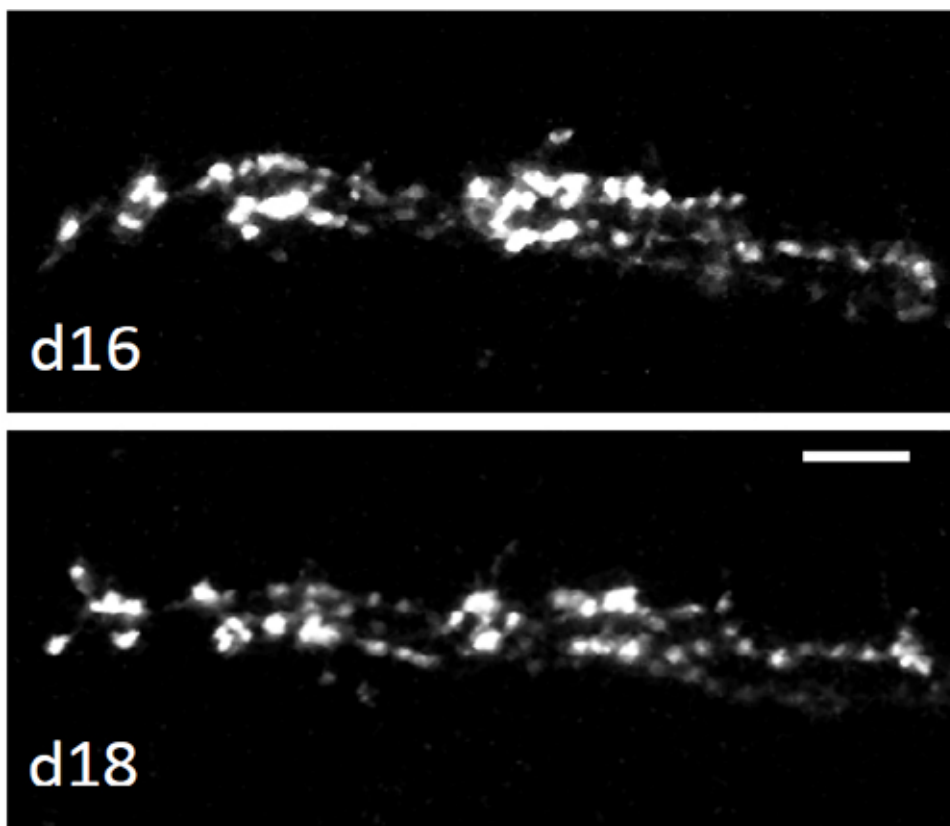


Figure 2. Climbing fibers labeling. The left panel shows an example of a CF labeled with Alexa Fluor 488 Dextran and visualized *in vivo* by TPF microscopy. Right panels display time-lapse images of the same CF from day 16 (d16) to d18. Scale bar, 10 μ m.

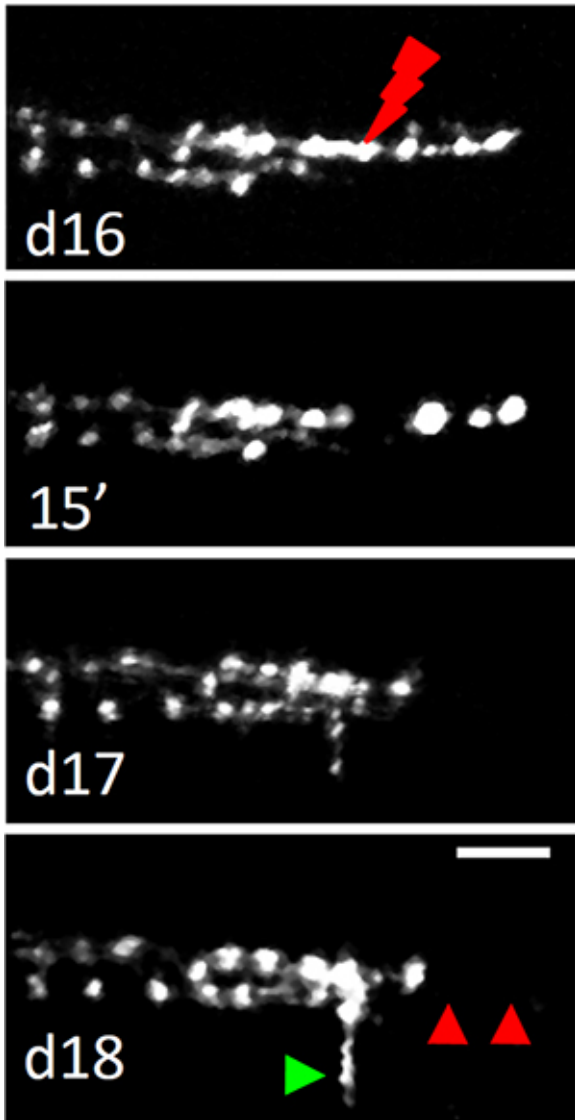


Figure 3. Laser axotomy on a single branch of a climbing fiber. The neuron was irradiated where the red arrow points on d16. Red arrowheads highlight the disappearance of the distal portion of the axon after laser axotomy (d18). A newly formed transverse branch is pointed out by the green arrowhead. Scale bar, 10 μ m.

Discussion

This protocol shows how to label neurons of the inferior olive with a fluorescent dye. Subsequently, the method to perform a cranial window on the cerebellar cortex is described. This technique provides optical access to the terminal portion of olivocerebellar neurons, the climbing fibers. Unfortunately, the outcome of both labeling and craniotomy surgery is quite low even in the hands of skilled operators (usually 1 out of 3 mice is labeled, and 1 out of 3 cranial windows remains clear after 1-2 weeks).

The procedure to perform laser axotomy in living mice is then presented. This method allows dissecting fluorescent neurons in targeted sites. While commonly used injury paradigms, either by mechanical severing or the use of chemicals, cause massive disruption of brain tissue, the key strength of this model is the high spatial confinement and specificity. Indeed, previous studies showed that single spines can be ablated while sparing the structural integrity of the parent dendrite⁵; moreover, single axonal branches can be disrupted avoiding the formation of a persistent glial scar⁶. The degeneration process can be then followed in real-time, as well as eventual remodeling of the injured neuron. This method is therefore a powerful tool to study the basic mechanism of axonal structural plasticity *in vivo*.

The possibility of dissecting selected structures depends to a first approximation on the depth of the structure and on its fluorescence emission intensity. Although two-photon microscopy allows imaging neurons up to 600-800 μ m deep, we found that the nanosurgery is limited to the first layers of the cortex (up to 300 μ m).

In this protocol laser axotomy was targeted to cerebellar climbing fibers, but it can be used to dissect any fluorescent structure in live brain. Laser irradiation has been used to dissect single neuronal cell bodies, dendritic branches, axons or single spines of GFP-labeled pyramidal neurons in the cortex of transgenic mice^{5,8,9,23}.

Disclosures

We have nothing to disclose.

Acknowledgements

We would like to thank Erica Lorenzetti for technical assistance on the injections and Irene Costantini for making figure 1. The research leading to these results has received funding from LASERLABEUROPE (Grant 284464, European Commission's Seventh Framework Programme). This research project has also been supported by the Italian Ministry for Education, University and Research in the framework of the Flagship Project NANOMAX and by Italian Ministry of Health in the framework of the "Stem Cells Call for Proposals." This work is part of the research activities of the European Flagship Human Brain Project and has been carried out in the framework of the International Center of Computational Neurophotonics foundation supported by "Ente Cassa di Risparmio di Firenze".

References

1. Strata, P., & Rossi, F. Plasticity of the olivocerebellar pathway. *Trends Neurosci.* **21**, 407-413, doi S0166-2236(98)01305-8 [pii] (1998).
2. Carulli, D., Buffo, A., & Strata, P. Reparative mechanisms in the cerebellar cortex. *Prog Neurobiol.* **72**, 373-398, doi 10.1016/j.pneurobio.2004.03.007S0301008204000413 [pii] (2004).
3. Zipfel, W., Williams, R., & Webb, W. Nonlinear magic: multiphoton microscopy in the biosciences. *Nature Biotechnology.* **21**, 1369-1377, doi 10.1038/nbt899 (2003).
4. Helmchen, F., & Denk, W. Deep tissue two-photon microscopy. *Nature methods.* **2**, 932-940, doi 10.1038/nmeth818 (2005).
5. Sacconi, L. *et al.* In vivo multiphoton nanosurgery on cortical neurons. *J Biomed Opt.* **12**, 050502, doi 10.1117/1.2798723 (2007).
6. Allegra Mascaro, A. L. *et al.* In vivo single branch axotomy induces GAP-43-dependent sprouting and synaptic remodeling in cerebellar cortex. *Proc Natl Acad Sci U S A.* **110**, 10824-10829, doi 10.1073/pnas.1219256110 (2013).
7. Ylera, B. *et al.* Chronically CNS-injured adult sensory neurons gain regenerative competence upon a lesion of their peripheral axon. *Curr Biol.* **19**, 930-936, doi 10.1016/j.cub.2009.04.017S0960-9822(09)00974-9 [pii] (2009).
8. Canty, A. J. *et al.* In-vivo single neuron axotomy triggers axon regeneration to restore synaptic density in specific cortical circuits. *Nat Commun.* **4**, 2038, doi 10.1038/ncomms3038ncomms3038 [pii] (2013).
9. Canty, A. J. *et al.* Synaptic elimination and protection after minimal injury depend on cell type and their prelesion structural dynamics in the adult cerebral cortex. *J Neurosci.* **33**, 10374-10383, doi 10.1523/JNEUROSCI.0254-13.201333/25/10374 [pii] (2013).
10. Waller, A. Experiments on the Section of the Glossopharyngeal and Hypoglossal Nerves of the Frog, and Observations of the Alterations Produced Thereby in the Structure of Their Primitive Fibres. *Philosophical Transactions of the Royal Society of London.* **140**, 423-429, doi 10.1098/rstl.1850.0021 (1850).
11. Hilliard, M. A. Axonal degeneration and regeneration: a mechanistic tug-of-war. *J Neurochem.* **108**, 23-32, doi 10.1111/j.1471-4159.2008.05754.xJNC5754 [pii] (2009).
12. Kerschensteiner, M., Schwab, M. E., Lichtman, J. W., & Misgeld, T. In vivo imaging of axonal degeneration and regeneration in the injured spinal cord. *Nat Med.* **11**, 572-577, doi nm1229 [pii]10.1038/nm1229 (2005).
13. Luo, L., & O'Leary, D. D. Axon retraction and degeneration in development and disease. *Annu Rev Neurosci.* **28**, 127-156, doi 10.1146/annurev.neuro.28.061604.135632 (2005).
14. Chauvet, N., Prieto, M., & Alonso, G. Tanycytes present in the adult rat mediobasal hypothalamus support the regeneration of monoaminergic axons. *Exp Neurol.* **151**, 1-13, doi S0014-4886(98)96784-X [pii]10.1006/exnr.1998.6784 (1998).
15. Morrison, E. E., & Costanzo, R. M. Regeneration of olfactory sensory neurons and reconnection in the aging hamster central nervous system. *Neurosci Lett.* **198**, 213-217, doi 030439409511943Q [pii] (1995).
16. Cafferty, W. B., McGee, A. W., & Strittmatter, S. M. Axonal growth therapeutics: regeneration or sprouting or plasticity? *Trends Neurosci.* **31**, 215-220, doi 10.1016/j.tins.2008.02.004S0166-2236(08)00088-X [pii] (2008).
17. Svoboda, K., & Yasuda, R. Principles of Two-Photon Excitation Microscopy and Its Applications to Neuroscience. *Neuron.* **50**, 823-839, doi (2006).
18. Feng, G. *et al.* Imaging neuronal subsets in transgenic mice expressing multiple spectral variants of GFP. *Neuron.* **28**, 41-51, doi (2000).
19. Tomomura, M., Rice, D. S., Morgan, J. I., & Yuzaki, M. Purification of Purkinje cells by fluorescence-activated cell sorting from transgenic mice that express green fluorescent protein. *Eur J Neurosci.* **14**, 57-63, doi ejn1624 [pii] (2001).
20. De Paola, V., Arber, S., & Caroni, P. AMPA receptors regulate dynamic equilibrium of presynaptic terminals in mature hippocampal networks. *Nat Neurosci.* **6**, 491-500, doi 10.1038/nn1046nn1046 [pii] (2003).
21. Holtmaat, A., & Svoboda, K. Experience-dependent structural synaptic plasticity in the mammalian brain. *Nature reviews. Neuroscience.* **10**, 647-658, doi 10.1038/nrn2699 (2009).
22. De Paola, V. *et al.* Cell type-specific structural plasticity of axonal branches and boutons in the adult neocortex. *Neuron.* **49**, 861-875, doi 10.1016/j.neuron.2006.02.017 (2006).
23. Allegra Mascaro, A., Sacconi, L., & Pavone, F. Multi-photon nanosurgery in live brain. *Frontiers in neuroenergetics.* **2**, 21, doi 10.3389/fnene.2010.00021 (2010).
24. Rossi, F., van der Want, J., Wiklund, L., & Strata, P. Reinnervation of cerebellar Purkinje cells by climbing fibres surviving a subtotal lesion of the inferior olive in the adult rat. II. Synaptic organization on reinnervated Purkinje cells. *The Journal of comparative neurology.* **308**, 536-554, doi 10.1002/cne.903080404 (1991).
25. Carulli, D., Buffo, A., & Strata, P. Reparative mechanisms in the cerebellar cortex. *Progress in neurobiology.* **72**, 373-398, doi 10.1016/j.pneurobio.2004.03.007 (2004).

26. Grasselli, G., Mandolesi, G., Strata, P., & Cesare, P. Impaired sprouting and axonal atrophy in cerebellar climbing fibres following *in vivo* silencing of the growth-associated protein GAP-43. *PLoS One*. **6**, e20791, doi 10.1371/journal.pone.0020791PONE-D-11-02774 [pii] (2011).
27. Nishiyama, H., Fukaya, M., Watanabe, M., & Linden, D. J. Axonal motility and its modulation by activity are branch-type specific in the intact adult cerebellum. *Neuron*. **56**, 472-487, doi S0896-6273(07)00708-8 [pii]10.1016/j.neuron.2007.09.010 (2007).
28. Shinoda, Y., Sugihara, I., Wu, H. S., & Sugiuchi, Y. The entire trajectory of single climbing and mossy fibers in the cerebellar nuclei and cortex. *Prog Brain Res*. **124**, 173-186, doi S0079-6123(00)24015-6 [pii]10.1016/S0079-6123(00)24015-6 (2000).
29. Strata, P., Tempia, F., Zagrebelsky, M., & Rossi, F. Reciprocal trophic interactions between climbing fibres and Purkinje cells in the rat cerebellum. *Prog Brain Res*. **114**, 263-282, doi (1997).
30. Mostany, R., & Portera-Cailliau, C. A craniotomy surgery procedure for chronic brain imaging. *J Vis Exp.* (12), doi 10.3791/680680 [pii] (2008).